A UNIVERSAL POWER ELECTRONIC INTERFACE FOR DISTRIBUTED GENERATION AND ELECTRIC VEHICLES

Yi Lu
Zhejiang Electric Power Test & Research Institute – China
luyi.zeptri@gmail.com

Xiao Ming Huang
Zhejiang Electric Power Test & Research Institute – China
huang_xiaoming@zj.sgcc.com.cn

Henry Wu
University of Liverpool – U. K.
q.h.wu@liv.ac.uk

ABSTRACT

The paper introduces a novel power-electronic based component for the power distribution network. The device serves as a universal interface between the distribution system and any user network which may contain distributed generation (DG) units. The power electronic interface utilizes the batteries inside electric vehicles for energy storage as well as an energy buffer layer. Therefore, it can smooth out the output power variation of the DG units. It also can charge electric vehicles with renewable energy. The circuit schematic and principle of operation is presented in the paper. The control strategy and some simulation results will be discussed in detail. The design considerations of a 50kVA prototype will be presented as well.

INTRODUCTION

The Chinese government recently published a series of policies to lower carbon emissions and support the development of Renewable Energy Resource (RES). As a result, the Zhejiang Electric Power Corporation recently received hundreds of applications of small wind turbines and photovoltaic for grid connection. These distributed generation (DG) units pose great challenges to local utility companies. Unlike conventional fossil power plants, the power generated by wind turbine or photovoltaic are largely determined by weather conditions. The unpredictability of RES means a higher cost for balancing the electricity grid and maintaining reserve capacity [1]. Small and medium sized DG units mostly use asynchronous generators which require reactive power support from the grid [2]. Some DG units connect to the grid via a DC-AC interface, which may contribute to higher harmonics [3].

On the other hand, the State Grid Corporation of China is accelerating the establishment of charging stations/spots in major cities. Alone in Zhejiang province, 18 charging stations and 500 charging spots will be set up by 2012. By the year 2015, 500 charging stations will be built in Zhejiang province, with the aim of supporting the country's "Energy efficient and new energy vehicle program" [4]. The rapid growing numbers of electric vehicles charge during peak hours could add an additional load to the grid. To tackle these issues, a universal power electronic interface (UPI) is developed to serve as a gateway between any DG units/electric vehicles and the grid.

CIRCUIT SCHEMATIC

As shown in Fig. 1, the device is consisted of a Utility-Side Module (USM), a Custom-Side Module (CSM), and an Electric Vehicle Module (EVM) along with a smart meter, battery units, and a control system.

The USM and CSM are two identical Voltage Source Converters (VSC) [5], which consist of 6 Insulated-Gate Bipolar Transistors (IGBT), AC filters, a separating transformer, a shunt capacitor and switches. The EVM comprise a buck-boost chopper, LC filters, fuses and switches.

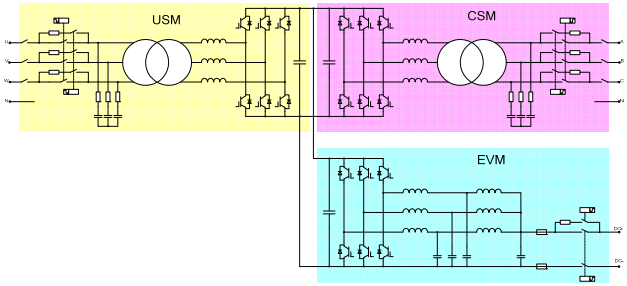

Figure 1. The main circuit schematic of the UPI

The USM and CSM connect the distribution network and consumer side network respectively. Both the USM and CSM can supply or absorb active and reactive power from the grid. Therefore, the UPI controls the active power exchange between the grid and the consumer. The capability of supplying dynamic reactive power enables USM to support the voltage stability of the local distribution grid. Similarly, the CSM can provide dynamic voltage support to the consumer side network. The EVM connects the electric vehicles and controls the charge and discharge of the battery units. The EVM, CSM and USM are connected through a DC bus.

It is evident that the UPI separates any DG unit and the grid. The UPI can provide reactive power, fault current limiting, and power quality control to both the distribution grid and the consumer network. Batteries inside the device as well as any electric vehicles connect to the device can be regarded as a small energy buffer. The device controls the power exchange among the grid, the load and electric vehicle. The power generated from DG can be used to charge electric vehicle or sold to the grid. If a power outage happens, the DG unit along with

the electric vehicle can continue to supply power to the load. When the DG unit cannot generate power due to weather conditions, the energy reserved in the batteries and the electric vehicle can maintain the output power constant for a period of time to improve the grid stability. By controlling the USM, the grid operator can control the output power of the DG unit. Through this gateway device, any DG units can connect to grid asynchronously.

CONTROL STRATEGY

The control scheme of the universal power electronic interface is based on instantaneous reactive power theory and *d-q* current decoupling control strategy [6]. The main equations describing the principles for instantaneous reactive power theory and decoupling control are given as in Equation (1) and (2).

$$P = \frac{3}{2}u_{sq}i_q = \frac{3}{2}u_s i_q \quad (1)$$

$$Q = -\frac{3}{2}u_{sq}i_d = -\frac{3}{2}u_s i_d \quad (2)$$

where u_{sd} and u_{sq} are the d and q axis components of AC bus voltage in the synchronous frame, i_d and i_q are line currents. After Park transformation, u_{sd}=0, u_{sq}=u_s, according to instantaneous power theory, the active and reactive power output of converter can be achieved.

Equation (1) and (2) shows that when the system running in steady-state, the instantaneous active power is only related to *q*-axis current component and the instantaneous reactive power is mainly determined by *d*-axis current component. Base on the current feed-forward loop decoupling method, the control equations for ud and uq are as following:

$$\begin{cases} u_{cd} = -(k_p + \frac{k_i}{s})(i_d^* - i_d) + \omega L i_q + u_{sd} \\ u_{cq} = (k_p + \frac{k_i}{s})(i_q^* - i_q) + \omega L i_d + u_{sq} \end{cases} \quad (3)$$

where u_{cd} and u_{cq} are the converter input voltage, k_p and k_i are the proportional and integral parameters, w is the frequency and L is the inductance.

USM

The USM is designed to keep DC bus voltage constant. The control diagram is shown in Fig. 2, the difference between DC bus reference voltage U_{dref} and measured value U_d are fed into a PI regulator to achieve the reference value of active current component i_{1qref}. The reactive current components i_{1dref} can be set as zero. The reference current is compared with the measured current i_{1d} and i_{1q} on the *d-q* axis. The differences between them are again fed into PI regulators. The outcome is again compared with the measured grid voltage u_{s1d}, u_{s1q} to achieve the *d-q* components of the USM converter voltage u_{c1d}, u_{c1q}. Based on decoupling method, the calculated converter voltage on *d-q* axis can be easily transformed to *abc* coordinate system and then achieve the modulating signal for the Synchronized Pulse-Width Modulation (SPWM) control.

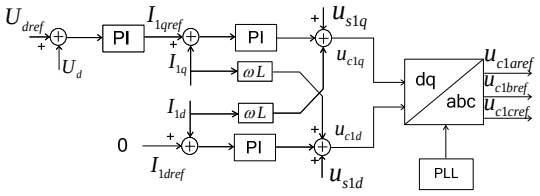

Figure 2 The control block diagram of the USM

CSM

The CSM functions as a constant voltage source. All other power electronics devices (photovoltaic inverters, etc.) inside the consumer network must correspond to the frequency and phase angle of the CSM.

The CSM adopts corresponding constant frequency and AC voltage control strategy [7], which is shown in Fig. 3. The difference between reference frequency f_{ref} and measured value f is fed into a PI regulator, to generate the reference of active current component I_{2qref}. Similarly, the difference between reference voltage of consumer side U_{s2ref} and measured value U_{s2} are used to produce the reference of the reactive current component I_{2dref}. The reference current is then compared with the actual measured current (I_{2q} and I_{2d}) on the *d-q* axis. The outcome is again compared with the measured consumer side voltage u_{s2d}, u_{s2q} to achieve the *d-q* components of the CSM converter voltage u_{c2d}, u_{c2q}, which can be transferred into abc coordinates to achieve SPWM signals.

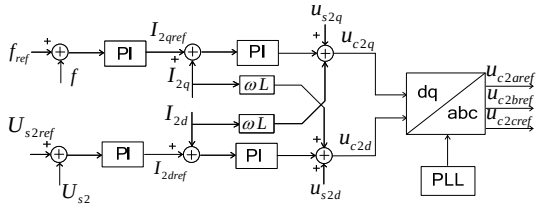

Figure 3 The control block diagram of the CSM

EVM

The control of EVM is based on the double close-loop control strategy. Fig. 4 shows the control diagram of discharging circuit. The inner loop is the discharging current control, while the outer is DC voltage control loop. The measured DC voltage U_d is compared with the reference DC voltage U_{dref} to generate the DC current reference signal. The latter is again compared with the measured DC current I_{d1} to produce required SPWM signal. The double close-loop control method of charging circuit is similar to the discharging circuit.

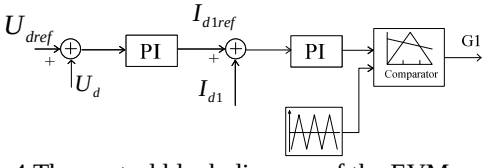

Figure 4 The control block diagram of the EVM

DESIGN CONSIDERATIONS

Main circuit parameters

Due to safety reasons, two separating transformers must be used at both the grid-side and consumer-side. Since there are not standard nominal voltages for the batteries in electric vehicles, the EVM must be able to charge at a wide voltage range of 35 to 300V. To keep the voltage ripples of the DC bus under 0.5%, the mark-space ratio of the buck-boost chopper should be set as high as possible. Therefore, the voltage level of the DC bus is chosen to be 360V; the ratio of the transformer is 380V/200V. A capacity of 50kVA is considered to be sufficient for most of the small and medium-size consumers. So the capacity of each module is set to be 50kVA. The other parameters of the UPI are shown in Table I.

Table I Main circuit parameters

	Parameter
Nominal Power	50kW
Nominal Reactive Power	-50kvar~50kvar
AC Input Voltage	380V±15%
Input Frequency	50Hz±5%
Stabilized Current Precision	≤±1%
Stabilized Voltage Precision	≤±1%
DC Current Ripple	≤±0.5%
Total Harmonic Distortion	<5%
Switching Time Between Charing & Discharging	<200ms
Over-flow Capacity	1min for 1.1×I_n, 10s for 1.2×I_n
Maximum Efficiency	≥93%
Cooling Method	Forced air cooling

Power electronics module

As shown in Table I, the UPI is required to have a 1.2 over-flow capacity, which means the maximum power for each module is 60kW. Considering the grid voltage floats between 304 and 456V, so that the maximum current level is 207A. The selected IGBT is model FF600R06ME3 from Infineon, which has an emitter current Ic of 600A. The margin of safety can be calculated as following:

Current Margin of Safety= $\frac{I_C}{\sqrt{2}I_e} = \frac{600A}{1.414 \times 207A} = 2$

where I_e is the over-flow current.

Since the USM and CSM have the identical structure, they share the same AC/DC module. As shown in Figure 5(a), the AC/DC power module integrates the IGBT, driving circuits, heat-sinks, fans, smoothing inductors and DC capacitor.

The EVM requires a separate DC/DC power module, as shown in Figure 5(b). The DC terminal of the IGBT connects the DC capacitor through a laminated bus bar, in order to minimize the stray inductance in the main circuit and suppress the switching over voltage. The driving circuit and the IGBT are integrated on the same board to minimize distance between them. The driving circuit receives firing signals from the control system via an optical fiber.

Control system

As shown in Figure 6, the control system communicates with the Battery Management System (BMS) via a Controller Area Network (CAN) bus. The information of battery status, grid-side and consumer-side voltage current are fed into the control system. Based on processing the information, the control system generates the firing signal for the IGBT. The control system communicates with the Human Machine Interface (HMI) via a RS232 link. The control system also receives commands from a backstage computer which is located at the local grid operator.

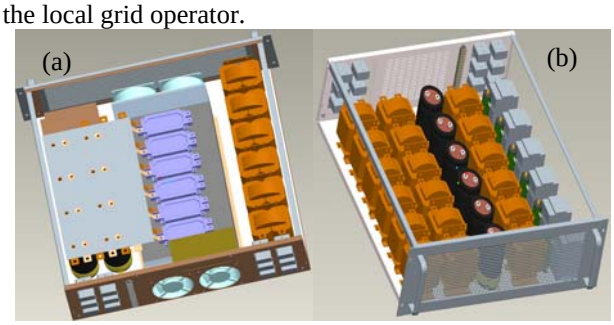

Figure 5. (a) The AC/DC power module. (b) the DC/DC power module.

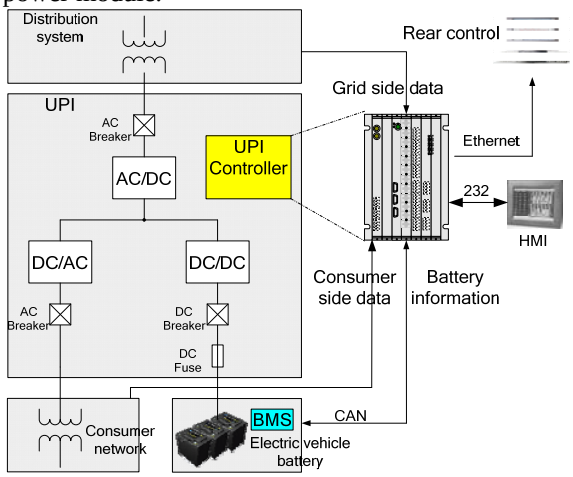

Figure 6. Schematic of the control system hardware.

SIMULATION RESULTS

Prior to the development of a prototype, some simulation studies were carried out in PSCAD/EMTDC environment. Assuming the distribution system is in steady state and the DG units on the consumer side is outputting power, so that on Figure 7(a), the active power flowing through the UPI initially is -0.1p.u. At 2.8s, the consumer switches on a large inductive load, Figure 7(a) illustrates that the active power flow reverses smoothly from -0.1p.u. to 0.2p.u., which indicates the consumer now absorb active power rather than supply it. Figure 7(b) shows that the reactive power flowing into the consumer side increases from 0.5p.u. to 0.78p.u. The active and reactive power re-achieves balance after around 0.1s.

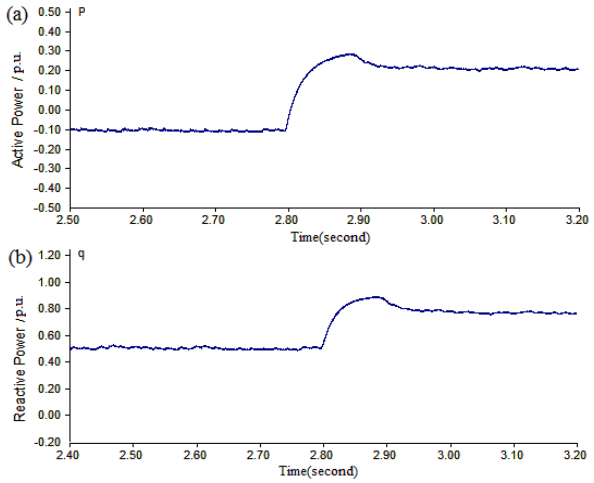

Figure 7. Active and reactive power flowing to the consumer side when load increases: (a) active power, (b) reactive power.

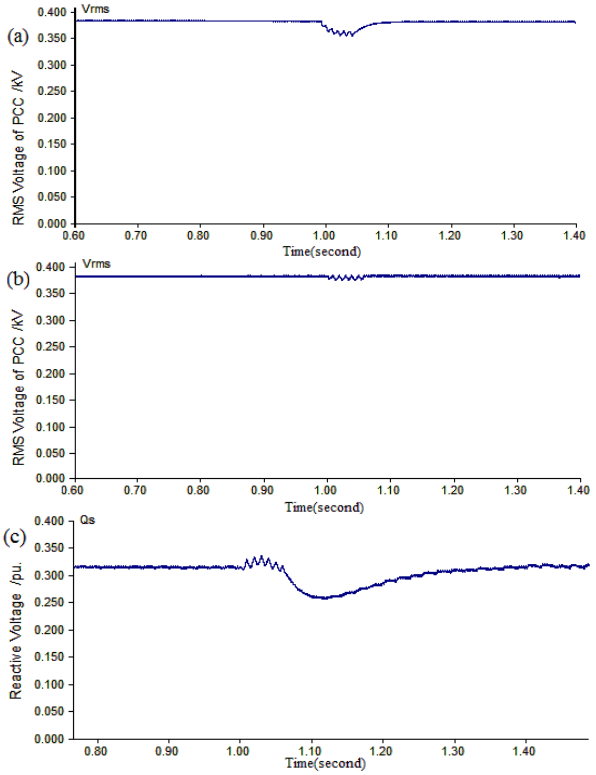

Figure 9. Simulation results when single-phase earthing fault occurs: (a) without UPI, (b) with UPI, (c) reactive power output of CSM.

Assuming a single-phase short-circuit fault occurred in the distribution grid about 1km away from the PCC, the effect on the voltage on the consumer-side with and without the UPI are illustrated in Figure 9. Figure 9(a) shows that without the UPI as an inter-connection device, severe voltage sag of the consumer network is observed when the fault occurs. When the consumer network is connect the system through the UPI, the voltage on the consumer side is almost free of disturbance, as shown in Figure 9(b). It is due to that the CSM increases the reactive power injection into the consumer side instantaneously with the fault occurs, as shown in Figure 9(c). Therefore, the voltage on the consumer side is strongly supported by the CSM.

CONCLUSION

The paper presents a novel component for the distribution system. The structure and operational principles of the interconnecting device are discussed in detail. The different control strategies for each module are proposed. Simulation in PSCAD/EMTDC was carried out. The results show that the UPI precisely controls the active power flowing bi-directionally between the consumer and the distribution system. The ability of reactive power compensation and voltage support is studied as well. The design issues of a prototype are also discussed.

REFERENCES

[1] L. Philison, 2000, "Distributed and Dispersed Generation Addressing the Spectrum of Consumer Needs," *Proceedings of 2000 IEEE Power Engineering Society Summer Meeting*, 1663-1665.

[2] P. Piagi, H. Lasseter Robert, 2006, "Autonomous control of Microgrids," *IEEE PES Meeting*, 1-8.

[3] A. A. Hinai and A. Feliachi, 2002, "Dynamic model of a microturbine used as a distributed generator", *Proc. of the 34th Southeastern Symposium*, 209-213.

[4] 2010, *The Twelfth "Five-Year Plan" of the Zhejiang Power Grid*, Zhejiang Electric Power Corporations., Hangzhou, China.

[5] Xiaoguang Wei, Guangfu Tang, Xiaoyun Wei, Yongning Chi, 2007 "Study of VSC-HVDC Controller to Mitigate Voltage Fluctuation Caused by Wind Farm Integration," *Transactions of China Electrotechnical Society*, Vol. 22, 150-156.

[6] E. Spahic, G. Balzer, 2005 "Offshore wind farms-VSC-based HVDC connection," *Power Tech, IEEE Russia* , 1-6.

[7] A. M. Abbas, P. W. Lehn, 2009 "A unified power delivery solution for integrating DER into distribution networks through VSC based DC system," *Power & Energy Society General Meeting, 2009. PES '09. IEEE*, 1-6.

Acknowledgments

The authors would like to acknowledge the Zhejiang Electric Power Corporation for supporting the research through project "The Key Technologies in a Smart Distribution Grid" (Contract No. ZDK082-2010) and for allowing this paper to be published.